9th Asia-Pacific Conference on Wind Engineering
Auckland, New Zealand
3-7 December 2017

Stratification Effects on Wind Characteristics over Two-Dimensional steep Hills

Tong WANG[1], Haotian DONG[2], Shuyang CAO[2], Fengli YANG[3], Hongjie ZHANG[3] and Yaojun GE[2]

[1]College of Civil Engineering
Shanghai Normal University, Shanghai 201418, China

[2]State Key Laboratory for Disaster Reduction in Civil Engineering
Tongji University, Shanghai 200092, China

[3]China Electric Power Research Institute, Beijing 100192, China

Abstract

Large-eddy simulations are performed to study a stably stratified incompressible flow with a linear temperature gradient past two sinusoidal two-dimensional steep hills with the maximum slope angles of 12 ºand 32 ºrespectively. The simulated Reynolds number is around Re=1370 based on the hill height *h* and the mean inlet velocity U_{mean}. Simulations are carried out for several stratification numbers *k* from 0 to 0.04 with respect to the buoyancy frequency *N*, the mean inlet velocity U_{mean} and the hill height *h*. Inflow turbulence and surface roughness are not considered for simplicity. Results show that stratification decreases the near-ground speedup over the upslope, while increases it in the wake. However, the near-ground turbulence intensity is increased around the hills and decreased downstream far away from the hills.

Introduction

Flow over complex terrain has become a hot research topic in the field of wind engineering for the past several decades due to the increased interest in wind energy applications and the increasing number of factories and wind-sensitive structures in mountainous region. Identifying positions with accelerations in the mean wind and their magnitudes is crucial for wind turbine siting, whereas changes to both the mean wind and turbulence are important when predicting pollutant dispersion or estimating wind loads on structures in hilly areas. Many investigations have studied the neutral flow over an isolated hill, which is usually a start point in research on flow over complex terrain, such as the work of Jackson and Hunt [6], Mason and King [8], Neff and Meroney [10], Cao and Tamura [1] and Wang et al. [16].

However, the atmospheric boundary layer is in nature not neutral but stratified because of the non-uniform temperature distribution and the gravitational force which tends to lower the heaviest fluid and to raise the lightest. Stratified flow past a hill may exhibit fully different characteristics from those by neutral one. A great effort has been devoted to studying the stratified flow over complex terrain. Smith [13] formulated and solved analytically a steady-state two-dimensional (2D) nonlinear problem of stratified airflow above a mountain ridge in the hydrostatic approximation. Gutman [4] generalized the Smith's solution by retaining a term in the continuity equation, which took into account the decrease of air density with height. Davies et al. [2] developed and tested a 2D downslope wind model which is formulated using a terrain-following coordinate system. Except for the above analytical studies, several field measurements were conducted. Mobbs et al. [9] observed the near-surface flow field across and downwind of a mountain range on the Falkland Island, South Atlantic. Oltmanns et al. [11] presented systematic study of the downslope wind events in Ammassalik in southeast Greenland. Besides, numerous numerical studies were also done. Sun [14] simulated the severe downslope windstorm occurred during 11 and 12, 1972 in the lee of Rocky Mountains. Leo et al. [7] carried out field measurements to study the dividing streamline concept. In addition, many experiments and numerical simulations were also implemented. Hunt and Snyder [5] experimentally compared stably and neutrally stratified flow over a model 3D hill. And Ding et al. [3] carried large-eddy simulation (LES) to examine the experimental work of Hunt and Snyder [5]. Ross et al. [12] made a comparison of numerical and experimental results for flow over 2D hills in both neutral and stably stratified flow. Wan et al. [15] tested three different sub-grid scales (SGS) models by comparing their LES results of stably stratified flow over a 2D steep hill with the experimental results of Ross et al. [12]. Most of the above works has been devoted to validating and revising the analytical or empirical models. Whereas there has been less research focusing on stratification effects on speedup and turbulence intensity.

In the present paper, we carry out large-eddy simulation to study stratification effects on wind characteristics over 2D steep hills with focus on speedup and turbulence intensity. In order to directly present the stratification effects and also to simplify the calculation and analysis, inflow turbulence and surface roughness are not taken into account. In addition, simplifications are introduced to define the stratification as the condition that inflow temperature rises linearly in the vertical direction, which is equivalent to a linear density gradient according to Boussinesq approximation. The stratification strength can be defined by the internal Froude number Fr or by a stratification number *k* defined by

$$k = \frac{Nh}{U_{\mathrm{mean}}\pi} \tag{1}$$

$$N^2 = -\frac{g}{\rho_0}\frac{\partial \rho}{\partial y} = \frac{g}{\theta_0}\frac{\partial \theta}{\partial y} \tag{2}$$

where *N* is the Brunt–Väisälä frequency which is also known as the buoyancy-driven oscillation frequency of a fluid parcel, U_{mean} the mean velocity at the inlet and *h* the height of the hill as shown in figure 2, *g* the gravity acceleration, ρ and ρ_0 the flow density and its reference value, θ and θ_0 the potential temperature and its reference value, and *y* the height from the ground. The present definition of stratification number is different from that given by Ding et al. [3], which is based on the free-stream velocity U_∞ and the hill height *h*. With a constant gradient-wind level, the free-stream velocity cannot reflect effects of the vertical scale of the computational domain. In order to clarify the stratification effect, the simulations were carried out for several stratification numbers, *k*=0, 0.03, 0.036 and 0.04.

Problem Formulation and Numerical Setup

The hills concerned had a sinusoidal shape defined by

$$y = h\cos^2\left(\frac{\pi x}{2L}\right) \tag{3}$$

where h is the hill height and L half the hill length, as shown in figure 1. Two hill shapes were considered: L=7.5h and L=2.5h, with maximum slope angles of 12 ºand 32 º, respectively.

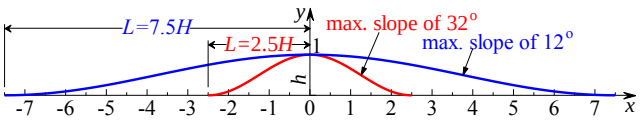

Figure 1. Hill shapes concerned

In the present study, the linearly-stratified flow is treated as an incompressible fluid simplified by Boussinesq approximation, where ρ=ρ_0 is constant in all solved equations, except for the buoyancy term in the momentum equation,

$$(\rho-\rho_0)g \approx -\rho_0(\alpha T-\alpha T_0)g \tag{4}$$

where T and T_0 are the local and reference temperature, respectively, and α is the thermal expansion coefficient. From Boussinesq approximation, the constant density gradient is equivalently replaced by a linear gradient of temperature. The accuracy of the Boussinesq approximation is sufficient as long as the changes in density are small, namely

$$\alpha T-\alpha T_0 << 1 \tag{5}$$

In the simulation, a high-Rayleigh-number condition is assumed, so the heat transfer is primarily in the form of convection, corresponding to a condition of buoyancy-force-driven natural convection. In addition, changes of fluid thermal properties are neglected, which means that the viscosity coefficient, the thermal conductivity and the specific heat are treated as constant. Equations (6)-(8) show the filtered Boussinesq equations for LES,

$$\frac{\partial \bar{u}_i}{\partial x_i} = 0 \tag{6}$$

$$\frac{\partial \bar{u}_i}{\partial t}+\bar{u}_j\frac{\partial \bar{u}_i}{\partial x_j} = -\frac{1}{\rho_0}\frac{\partial \bar{p}}{\partial x_i}+\frac{\mu}{\rho_0}\frac{\partial^2 \bar{u}_i}{\partial x_i \partial x_j}-\frac{\partial \tau_{ij}}{\partial x_j} - \alpha g_i(T-T_0) \tag{7}$$

$$\frac{\partial \bar{T}}{\partial t}+\bar{u}_j\frac{\partial \bar{T}}{\partial x_j} = \kappa\frac{\partial^2 \bar{T}}{\partial x_i \partial x_j}-\frac{\partial \tau_{Tj}}{\partial x_j} \tag{8}$$

in which u_i=(u,v,w) and x_i=(x,y,z) represent the velocity and coordinate components, the over-bar denotes the space filtered quantities, and κ represents the thermal diffusivity. The SGS stresses τ_{ij} are

$$\tau_{ij} = \overline{u_i u_j}-\bar{u}_i\bar{u}_j \tag{9}$$

And the sub-gird thermal fluxes τ_{Tj} are defined by

$$\tau_{ij}-\frac{1}{3}\delta_{ij}\tau_{kk} = -2\nu_{SGS}\bar{S}_{ij} = \nu_{SGS}\left(\frac{\partial \bar{u}_i}{\partial x_j}+\frac{\partial \bar{u}_j}{\partial x_i}\right) \tag{10}$$

$$\tau_{Tj} = -\frac{\nu_{SGS}}{\mathrm{Pr}}\frac{\partial \bar{T}}{\partial x_j} \tag{11}$$

$$\nu_{SGS} = (C_S\bar{\Delta})^2|\bar{S}| \tag{12}$$

where the turbulent Prandtl number is Pr=0.85; $\bar{S}_{ij}$ is the strain rate tensor and $|\bar{S}| = \sqrt{2\bar{S}_{ij}\bar{S}_{ij}}$; ν_{SGS} is the SGS eddy viscosity; the Smagorinsky constant is C_S=0.1 and the grid filter size is $\bar{\Delta} = (\Delta x\Delta y\Delta a)^{1/3}$; for near-wall girds, $\bar{\Delta}$ is replaced by a mixing length $\bar{\Delta}$) in which k is the von Karman constant and d is the distance to the closest wall.

The simulation was carried out with the aid of the Fluent© package. The options of numerical methods offered by Fluent© are selected carefully in order to achieve reliable simulation results. The spatial discretization was based on the Finite Volume Method (FVM). The least squares cell-based gradient evaluation was applied to obtain the gradients. The Pressure Staggering Option scheme, which was suitable for high Rayleigh number natural convection flow, was applied for pressure discretization. For spatial differencing of the convection term, a bounded central differencing scheme was used to avoid unphysical oscillations while providing good accuracy for energy discretization. For temporal discretization, the second order implicit formulation was chosen. The PISO (Pressure Implicit with Splitting of Operator) algorithm was applied as the pressure-velocity coupling scheme.

The computational domain is illustrated in Figure 2. The vertical and spanwise lengths are L_y=25h and L_z=8h, respectively, resulting in a blockage ratio of 4%. The distances before and after the hill are L_b=30h and L_a=30h, respectively.

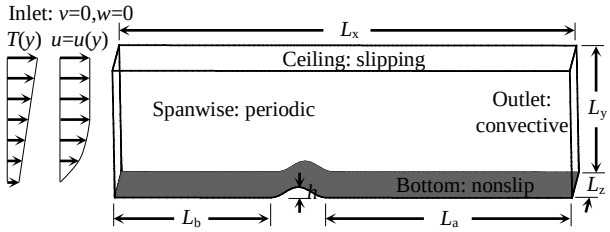

Figure 2. Graphic of the computational domain and boundary conditions

Boundary conditions are also shown in figure 2. A no-slip condition and a zero heat flux condition were imposed for the bottom, a slipping condition for the ceiling, a periodic condition for the spanwise and a convective condition for the outlet. The temperature condition for inlet is set as a stationary vertically linear temperature distribution, and the velocity conditions were as v=0, w=0 and

$$u(y) = \left(\frac{u_*}{\kappa}\right)\ln\left(\frac{y}{y_0}\right), \text{ for } y\le 2.5h \tag{13}$$

with gradient-wind level being 2.5h, where u_* is the friction velocity, κ the Karman constant, y_0 the surface roughness length. The Reynolds number is around Re=1370 based on the hill height h and the mean inlet velocity U_{mean}.

Several structural grid systems were tested to examine the mesh dependence, and two fine grid systems were chosen for the 12 º and 32 ºhill (Figure 3), respectively. L_z was uniformly discretised into 16 cells for both the above two grid systems. L_y was discretised into 100 cells with the first grid near ground given empirically by $\sqrt{\ }$. The grid size stretched upward in the

vertical direction. L_x was divided into 550 and 480 cells for the 12 °and 32 °hill with the minimum grid of 0.05h and 0.03h over the hilltop, respectively. And also the grid size stretched upstream and downstream in the longitudinal direction (Figure 3). The non-dimensional time step, defined by $\Delta t = \Delta t' U_{mean}/h$ where $\Delta t'$ is the dimensional time step, was set as Δt =0.03 and 0.015 for the 12 °and 32 °hill, respectively. The Courant number remained below 1 in all calculation cases.

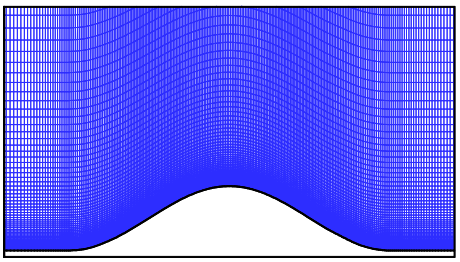

Figure 3. Grid around the 32 °hill

Numerical Validation

In order to validate the present simulation, instantaneous and time-averaged flow around the 32 °hill in neutral flow obtained by the present numerical simulation were compared with those of previous numerical studies. Fig. 4 illustrates 2D snapshots of instantaneous and time- and spanwise-averaged streamlines of flow field around the hill in the present neutral-flow simulation. A series of vortex shedding and a strong reverse flow of the separated shear layer behind the hill, which are the well-known flow features of the steep hill, can be found in Figure 4a. The length of separation bubble as shown in Figure 4b is around 12.9h which is nearly the same as that given by Wang et al. [16] with the same Reynolds number. Figure 5 compares the time- and spanwise-averaged velocity profiles over the hill at several positions along the streamwise direction with those of Wang et al. [16], and a good agreement is found.

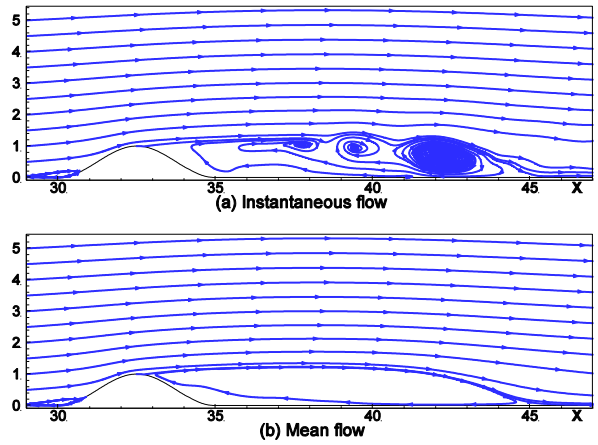

Figure 4. Instantaneous and time- and spanwise-averaged streamlines of flow field around the 32 °hill in neutral flow

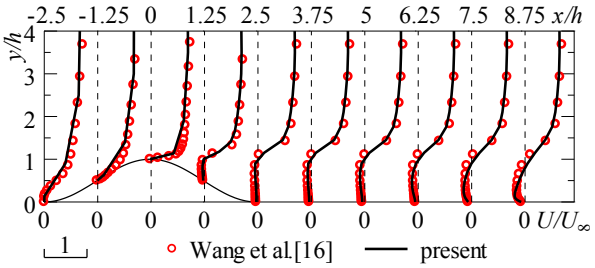

Figure 5. Time- and spanwise-averaged velocity profiles for the 32 °hill

Stratification effects on Wind Characteristics

Figure 6 shows the time- and spanwise-averaged velocity and *rms* profiles at a series of position over the 12 °hill along the streamwise direction. Only the results for cases of k=0, 0.036 and 0.04 are presented. Clearly, stratification has strong influence on wind statistics especially in the wake where the mean velocity near ground is increased (Figure 6a), resulting in a smaller recirculation zone. However, over the upslope, stratification slightly decreases the near-ground mean velocity. As shown in Figure 6b, the near-ground turbulence intensity around the hill is enlarged while reduced downstream far away from the hill. And clearly, the higher the stratification number, the larger the effects.

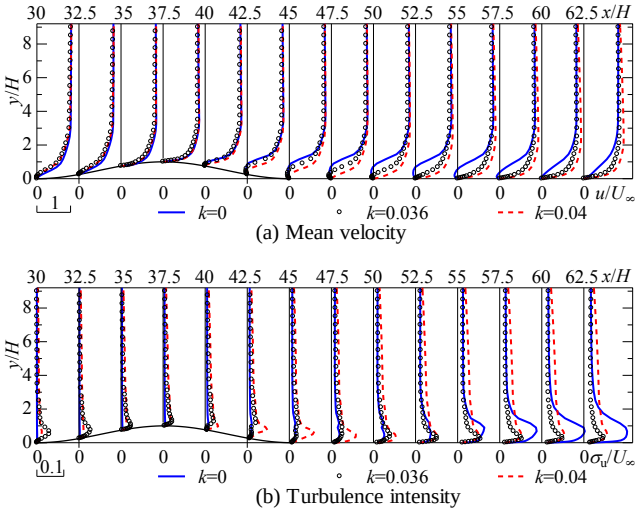

Figure 6. Turbulent statistics over the 12 °hill for k=0, 0.036 and 0.04

Figure 7 shows the time- and spanwise-averaged velocity and *rms* profiles at a series of position over the 32 °hill along the streamwise direction. Only the results for cases of k=0, 0.03 and 0.04 are presented. Like the 12 °hill, stratification has strong influence on wind statistics in the wake where the mean velocity near ground is increased and the recirculation zone shrinks. And also the stratification effects on flow statistics of the hill have

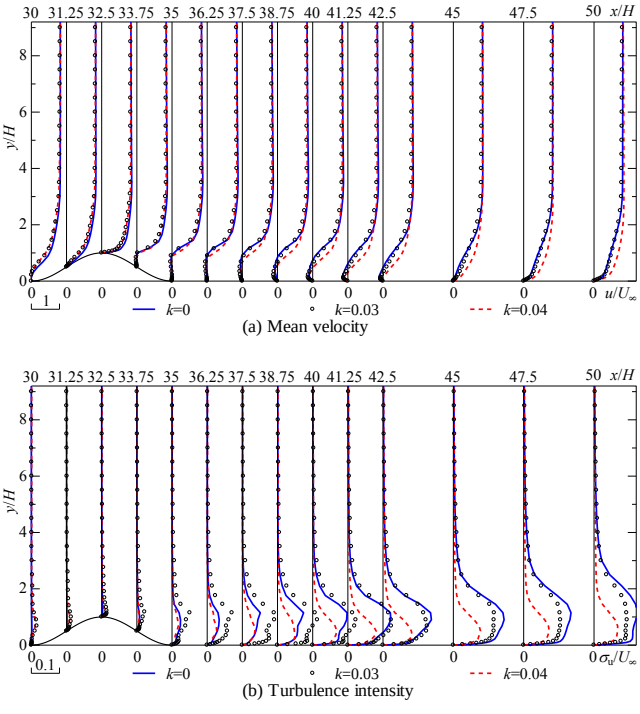

Figure 7. Turbulent statistics over the 32 °hill for k=0, 0.03 and 0.04

similar rules to those of the 12 ºhill. Compared with the 12 ºhill, the stratifications effect is smaller on mean velocity and larger on *rms*. In addition, the effect area is higher than that of the 12 ºhill, especially for *rms* (Figure 7b). Stratification effects on flow over hills are complicated and dependent on hill slope.

Conclusions

Large-eddy simulations are performed to study the stratification effects on wind characteristics over two kinds of sinusoidal two-dimensional steep hills with the maximum slope angles of 12 º and 32 º, respectively, without considering inflow turbulence and ground roughness. Stably stratified inflow condition is imposed at inlet, and the Boussinesq approximation is introduced to define the stratification as the condition that inflow temperature rises linearly in the vertical direction. The present numerical results show that stratification decreases the near-ground speedup over the upslope, while increases it in the wake. However, the near-ground turbulence intensity is increased around the hills and decreased downstream far away from the hills. The effect area is higher for the steeper hill. So it is necessary to consider the stratification effects in hilly areas with strong temperature gradient.

Acknowledgments

This work has been funded by the State Grid Corporation of China (The project name is Study on the Wind Load Characteristics and Tower Structures of Transmission Lines in the Strong Wind Regions under Extreme Environmental Conditions) and the National Natural Science Foundation of China (Grant No. 51508333).

References

[1] Cao, S. & Tamura, T., Effects of Roughness Blocks on Atmospheric Boundary Layer Flow over a Two-dimensional Low Hill with/without Sudden Roughness Change, *J. Wind Eng. Ind. Aerodyn.*, **95**, 2007, 679-695.

[2] Davies, T.D., Palutikof, J.P., Guo, X., Berkofsky, L. & Halliday, J., Development and Testing of a Two-Dimensional Downslope Wind Model, *Bound.-Lay. Meteorol.*, **73**, 1995, 279-297.

[3] Ding, L., Calhoun, R.J. & Street, R.L., Numerical Simulation of Strongly Stratified Flow over a Three-dimensional Hill. *Boundary-Layer Meteorol.*, **107**, 2003, 81-114.

[4] Gutman, L.N., Downslope Windstorms. Part I: Effect of Air Density Decrease with Height, *J. Atmos. Sci.*, **48**, 1991, 2545-2551.

[5] Hunt, J.C.R. & Snyder W.H., Experiments on Stably and Neutrally Stratified Flow over a Model Three-dimensional Hill, *J. Fluid Mech.*, **96**, 2006, 671-704.

[6] Jackson, P.S. & Hunt, J.C.R., Turbulent wind flow over a low hill, *Q. J. R. Meteorol. Soc.*, **101**, 1975, 929-955.

[7] Leo, L.S., Thompson, M.Y., Sabatino, S.D. & Fernando, H.J.S., Stratified Flow past a Hill: Dividing Streamline Concept Revisited, *Boundary-Layer Meteorol*., **159**, 2016, 611-634.

[8] Mason, P.J. & King, J.C., Measurements and Predictions of Flow and Turbulence over an Isolated Hill of Moderate Slope, *Q. J. R. Meteorol. Soc.*, **111**, 1985, 617-640.

[9] Mobbs, S.D., Vosper, S.B., Sheridan, P.F., Cardoso, R., Burton, R.R., Arnold, S.J., Hill, M.K., Horlacher, V. & Gadian, A.M., Observations of Downslope Winds and Rotors in the Falkland Islands, *Q. J. Roy. Meteor. Soc.*, **131**, 2005 , 329-351.

[10] Neff, D.E. and Meroney, R.N. (1998), "Wind-tunnel modeling of hill and vegetation influence on wind power availability", *J. Wind Eng. Ind. Aerodyn.*, **74-76**, 335-343.

[11] Oltmanns, M., Straneo, F., Moore, G.W.K. & Mernild, S.H., Strong Downslope Wind Events in Ammassalik, Southeast Greenland, *J. Climat.*, **27**, 2014, 977-993.

[12] Ross, A.N., Arnold, S., Vosper, S.B., Mobbs, S.D., Dixon, N. & Robins, A.G., A Comparison of Wind-tunnel Experiments and Numerical Simulations of Neutral and Stratified Flow over a Hill, *Boundary-Layer Meteorol*., **113**, 2004, 427-459.

[13] Smith, R.B., On Severe Downslope winds, *J. Atmos. Sci.*, 42, 1985, 2597-2603.

[14] Sun W.-Y., Numerical Study of Severe Downslope Windstorm, *Weather and Climate Extremes*, **2**, 2013, 22-30.

[15] Wan, F. & Port é-Agel, F., Large-Eddy Simulation of Stably-Stratified Flow Over a Steep Hill, *Boundary-Layer Meteorol*., **138**, 2011, 367-384.

[16] Wang, T., Cao, S. & Ge, Y., Effects of Inflow Turbulence and Slope on Turbulent Boundary Layers over Two-dimensional Hills, *Wind Struct.*, 19, 2014, 219-232.